Review | Vol. 16, No. 7 / 1 Jul 2026 / Optical Materials Express 2135

Optical Materials EXPRESS

Zeroth-order mode antennas enabled by near-zero-index metamaterials: from theory to applications [Invited]

YUE LI,[1,2,3,*] PENGYU FU,[1] ZIHENG ZHOU,[4] YONGJIAN ZHANG,[5] WENDI YAN,[1] MINGZHE HU,[1] SHUYU WANG,[1] PEIHANG LI,[1] XUAN LIU,[1] KAIFENG LI,[1] HANFEI BU,[1] AND XUXUAN LIN[1]

[1] *Department of Electronic Engineering, Tsinghua University, Beijing 100084, China*
[2] *Beijing National Research Center for Information Science and Technology, Tsinghua University, Beijing 100084, China*
[3] *State Key Laboratory of Space Network and Communications, Tsinghua University, Beijing 100084, China*
[4] *College of Physics and Information Engineering, Fuzhou University, Fuzhou 350108, China*
[5] *Unmanned System Research Institute, Northwestern Polytechnical University, Xi'an 710072, China*
[*] *lyee@tsinghua.edu.cn*

Abstract: Near-zero-index (NZI) metamaterials, characterized by an effective refractive index approaching zero, exhibit a near-zero propagation constant and an extremely large wavelength, resulting in fundamentally different wave dynamics. NZI media support nearly uniform phase and spatially coherent fields, enabling geometry-independent behavior and wave tunneling. These properties relax the coupling between geometry and electromagnetic response, offering a new way to overcome the limits of conventional electromagnetic devices. In antenna engineering, such decoupling challenges the conventional constraint that resonance and radiation characteristics are tied to structural dimensions, enabling new opportunities for antenna miniaturization and radiation control. In practice, NZI behavior is typically realized through zeroth-order modes (ZOMs), allowing antennas to achieve geometry-independent resonance with enhanced design flexibility. This review first outlines the fundamental electromagnetic properties of NZI metamaterials, then surveys the operating principles and representative designs of ZOM antennas across different platforms, including periodic structures, transmission-line loops, and waveguide-based configurations. Finally, we discuss key challenges such as loss, bandwidth, and system integration, and highlight future directions for NZI-enabled antenna engineering.

1. Introduction

Metamaterials and artificial electromagnetic media provide versatile platforms for manipulating electromagnetic waves beyond natural-material limits [1,2]. By tailoring effective permittivity and permeability, they enable access to unconventional parameter regimes and new mechanisms for wave control [3,4]. In this context, pioneering studies led by Professor Nader Engheta and others have driven the development of near-zero-index (NZI) metamaterials, significantly advancing the understanding of electromagnetic states with near-zero propagation constants, as shown in Fig. 1 [5–7]. Early concepts such as nihility and zero-parameter electromagnetics established the theoretical basis of NZI media [8–11], later formalized through systematic studies revealing anomalous tunneling and supercoupling effects [12–15]. Subsequent work extended NZI implementations to photonic crystals, optical frequencies, and integrated photonic platforms [16–21], while recent efforts have focused on tunable systems via photonic doping and the exploration of phenomena such as electromagnetic fluid behavior and energy-flow manipulation [22–33]. Physically, NZI metamaterials operate in a regime where the propagation constant approaches zero, yielding an effectively infinite wavelength and minimal phase variation. As a

#604768 https://doi.org/10.1364/OME.604768
Journal © 2026 Received 8 May 2026; revised 12 Jun 2026; accepted 12 Jun 2026; published 22 Jun 2026

Optical Materials EXPRESS

result, electromagnetic fields exhibit nearly uniform phase distributions and quasi-static spatial characteristics despite being time-harmonic. This mechanism weakens the dependence on propagation path and geometry, enabling a fundamental decoupling between structural size and electromagnetic response [27,34,35].

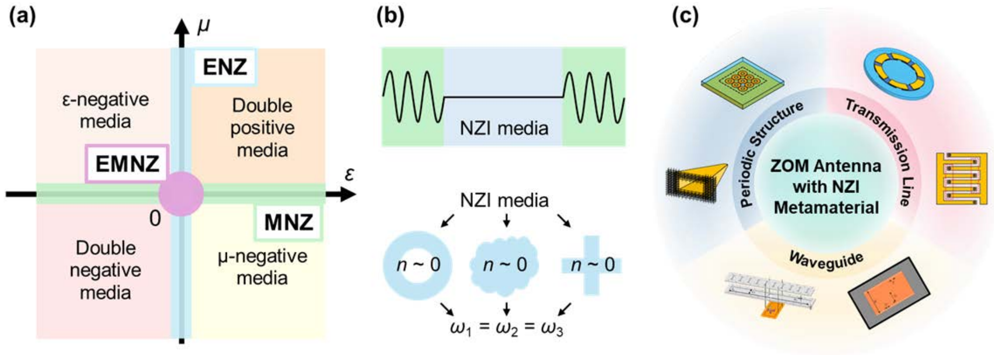

Fig. 1. Schematic illustration of NZI metamaterials. (a) Definition of NZI in refractive-index space. (b) Key electromagnetic properties of NZI. (c) ZOM-enabled antenna implementations [47,50]. Reproduced with permission. Copyright 2022, IEEE, and copyright 2024, IEEE.

Despite the clear theoretical promise of NZI metamaterials for geometry-frequency decoupling, realizing homogeneous NZI media in practice remains difficult. To address this, engineered finite structures have been developed to emulate near-zero propagation, among which zeroth-order modes (ZOMs) offer a practical solution. Under ZOM operation, the propagation constant approaches zero, suppressing phase variation and making resonance primarily determined by boundary conditions. This mechanism enables subwavelength resonance and greater design flexibility, serving as an effective realization of NZI behavior [36–38]. In this sense, ZOMs bridge fundamental NZI physics and practical electromagnetic devices. Such features are especially valuable in antenna systems, where resonance and radiation are typically constrained by electrical size [39–41]. By contrast, the near-zero phase variation of ZOMs relaxes this constraint, allowing more flexible control of antenna performance.

Building on these principles, several engineering approaches have been developed for ZOM-based antennas, including periodic structures enabling near-zero propagation via effective media, transmission-line designs achieving zeroth-order resonance through circuit tuning, and waveguide-based systems utilizing mode engineering for efficient radiation [42–47]. Despite notable progress in miniaturization and radiation control, challenges persist in loss, bandwidth, and system integration [48–51]. Moreover, the physical mechanisms and performance trade-offs across these approaches remain insufficiently unified. To clarify this, Fig. 2 outlines the development of NZI theory and key properties, along with their implications for antenna design. This review provides a physics-driven overview of ZOM antennas based on NZI metamaterials. We first introduce the fundamental properties of NZI media, then present a unified interpretation of ZOM formation, followed by a survey of representative designs. Finally, key challenges and future directions are discussed.

Optical Materials EXPRESS

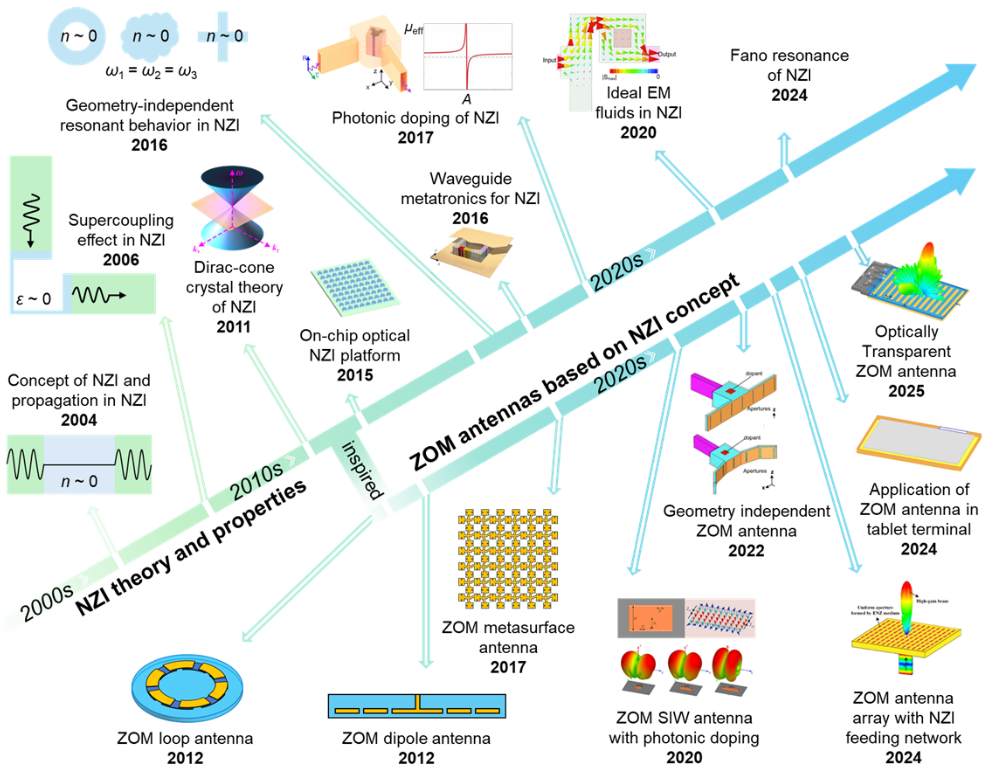

Fig. 2. **Timeline of the development of NZI metamaterials, their key physical properties, and NZI-inspired ZOM antenna applications** [10,12,16,17,23,27–29,33,34,36,37,44,48,50,51,77,107,113]. Reproduced with permission. Copyright 2019/2020/2024/2024/2025, IEEE, and copyright 2020/2022, Springer Nature, and copyright 2016/2017, Science, and copyright 2023, Willey.

2. Theory of antennas with near-zero-index metamaterials

2.1. Fundamental theory of NZI metamaterials

NZI metamaterials are electromagnetic media or engineered structures in which the effective refractive index approaches zero [5,6]. Since $n = \sqrt{\varepsilon_r \mu_r}$, a near-zero index can arise when either permittivity or permeability approaches zero, leading to three main categories: epsilon-near-zero (ENZ), mu-near-zero (MNZ), and epsilon-and-mu-near-zero (EMNZ) materials. Owing to this property, electromagnetic waves in NZI media exhibit highly unconventional responses.

First, according to the general expressions for the wavelength and phase velocity of electromagnetic waves in a medium [5,6]:

$$\lambda = \lambda_0/n = \lambda_0/\sqrt{\varepsilon_r \mu_r} \tag{1}$$

$$v_p = c/n = c/\sqrt{\varepsilon_r \mu_r} \tag{2}$$

When either the permittivity or permeability approaches zero, the wavelength and phase velocity tend to infinity. As a result, the wavelength inside a zero-index medium is significantly stretched, leading to negligible phase accumulation over a finite region. The electromagnetic field therefore exhibits quasi-static spatial behavior while remaining time-harmonic, giving rise to the characteristic of “temporal oscillation with spatial uniformity.”

Second, according to the general expression for the group velocity in an arbitrary linear and isotropic medium [52],

$$v_g = \frac{\partial \omega}{\partial k} = \frac{2c}{2\sqrt{\varepsilon_r \mu_r} + \omega\sqrt{\frac{\mu_r}{\varepsilon_r}}\frac{\partial \varepsilon_r}{\partial \omega} + \omega\sqrt{\frac{\varepsilon_r}{\mu_r}}\frac{\partial \mu_r}{\partial \omega}} \tag{3}$$

When either the relative permittivity ε_r or permeability μ_r approaches zero while the other parameter remains finite, the group velocity tends to zero due to divergence in its governing expression. As a result, ENZ and MNZ media exhibit vanishing group velocity, corresponding to the "slow-light effect" in optics [53]. Third, according to the expression for the intrinsic impedance of an electromagnetic wave,

$$\eta = \sqrt{\frac{\mu}{\varepsilon}} = \eta_0\sqrt{\frac{\mu_\mathrm{r}}{\varepsilon_\mathrm{r}}} \tag{4}$$

According to this expression, when both the relative permittivity ε_r and permeability μ_r approach zero, the intrinsic impedance assumes an indeterminate 0/0 form. In this limit, the impedance of an EMNZ medium is determined by the ratio $\varepsilon_\mathrm{r}/\mu_\mathrm{r}$ rather than their absolute values. By appropriately engineering this ratio, EMNZ media can in principle achieve impedance matching with arbitrary surrounding media [54]. Fourth, according to the wave equation in a passive, homogeneous, and isotropic medium,

$$\nabla^2 \mathbf{E} - \varepsilon\mu\frac{\partial^2}{\partial t^2}\mathbf{E} = 0 \tag{5}$$

$$\nabla^2 \mathbf{H} - \varepsilon\mu\frac{\partial^2}{\partial t^2}\mathbf{H} = 0 \tag{6}$$

In NZI materials, as the product $\varepsilon\mu = 0$, the effective propagation constant approaches zero, leading to a decoupling of spatial and temporal variations in the wave equation—referred to as the spatiotemporal decoupling property [6,34].

Furthermore, Nader Engheta and collaborators demonstrated that the effective permeability of an ENZ medium can be engineered through the introduction of nonmagnetic dielectric inclusions [22]. This concept was subsequently generalized and became widely known as photonic doping [23], whereby embedded dielectric inclusions effectively tailor the macroscopic electromagnetic response of an NZI medium:

$$\mu_\mathrm{eff} = 1 + \sum_\mathrm{d} \Delta\mu_\mathrm{d} \tag{7}$$

Through this mechanism, the effective permeability can be continuously tuned over a wide range. By tailoring the size and permittivity of the dopants, an ENZ medium can realize multiple electromagnetic responses, including EMNZ states.

More recently, NZI theory has been extended to describe global electromagnetic energy flow. In a lossless EMNZ medium, the Poynting vector vanishes, yielding $\nabla \cdot \mathbf{S} = 0$ and, under source-free TM excitation, $\nabla \times \mathbf{S} = 0$. Combined with the boundary condition $\mathbf{n} \cdot \mathbf{S} = 0$, this corresponds to a slip condition. These properties mirror those of an ideal fluid, forming the basis of the ideal electromagnetic fluid theory [27], later verified experimentally [28].

2.2. Properties of NZI metamaterials

The unusual responses of NZI metamaterials lead to several exotic phenomena, among which supercoupling is the most representative, first reported by Engheta and co-workers [12–15]. It describes electromagnetic waves propagating through ultranarrow ENZ channels with arbitrary

Optical Materials EXPRESS

bends and corners, showing minimal loss and weak dependence on geometry. This behavior arises from the effectively infinite wavelength and spatiotemporal decoupling in ENZ media. It has been extended to applications such as impedance transformation between transmission structures [55] and efficient wave transport in nanoscale optical waveguides [56].

With the development of photonic doping theory, supercoupling was extended beyond ultranarrow channels by tuning the effective permeability to zero, greatly broadening its scope. A representative example is the electromagnetic fiber, which supports efficient wave propagation along the E-plane under an EMNZ condition while preserving geometric flexibility [26]. Building on this, supercoupling has been expanded from single-port to multi-port systems, where transmission depends only on port width, enabling flexible power redistribution and impedance matching between modules [57,58]. More recently, these concepts have been generalized to multi-mode systems with bandwidth enhancement [29,59].

Another key consequence of spatiotemporal decoupling in NZI metamaterials is geometry-invariant behavior, where device dimensions and radiation characteristics are largely decoupled, and geometric variations do not significantly affect resonance or performance. This effect was first demonstrated by Nader Engheta's group, showing cavity resonances remain unchanged under substantial deformation [34]. Similar phenomena have been observed in thermal radiation systems, e.g., thermal rectification [60]. More recently, Yue Li's group extended this concept to antenna design, where it has become a defining feature of NZI antennas [35].

The effectively infinite wavelength and near-zero phase variation in NZI metamaterials lead to strong field enhancement, where energy redistributes across the entire region, resulting in pronounced field concentration [61]. This enables high sensitivity to permittivity variations, allowing transmission control via local perturbations such as dielectric inclusions [25], and has been applied to manipulate radiating and non-radiating modes for enhanced wave control [19].

NZI concepts have also been extended to the quantum domain, including directional quantum radiation, suppression of quantum fluctuations, and non-Hermitian photonic doping [24,62,63]. A unified framework further shows that emission and absorption can be suppressed in 3D systems but enhanced in lower dimensions [64]. Despite their diverse manifestations, many NZI phenomena originate from the near-zero propagation constant and the resulting suppression of phase accumulation. The associated stretched effective wavelength enables collective electromagnetic responses, forming the physical basis of supercoupling, geometry-invariant behavior, and unconventional radiation properties.

2.3. Implications of NZI metamaterials for antenna design

These unique electromagnetic properties offer a new paradigm for antenna design, enabling functionalities beyond conventional structures. A key feature is the decoupling of geometry and operating frequency, breaking the traditional size–resonance constraint [65]. Unlike conventional antennas, where frequency is determined by physical dimensions, NZI materials exhibit spatiotemporal decoupling, allowing resonators to maintain constant frequency under geometric variations [34]. This property extends to NZI antennas, enabling shape reconfiguration and flexible radiation control while preserving operating frequency [35].

Building on this decoupling property, NZI metamaterials enable flexible radiation control, particularly for wavefront shaping and pattern reconfiguration. This arises from their impedance-matching flexibility and geometry-independent behavior, allowing wave matching from arbitrary directions and geometry-tailored wavefront control [66]. NZI photonic crystals have also been used for directional quantum emission, and, combined with bound states in the continuum, can generate zero-phase planar wavefronts with enhanced directivity [62].

Extending these concepts to the microwave regime enables reconfigurable antennas. With operating frequency decoupled from the aperture, radiation patterns can be tuned via geometric modifications without shifting resonance. In particular, ENZ modes provide nearly uniform amplitude and phase distributions, enabling low-sidelobe two-dimensional radiation patterns through appropriate element spacing [67].

In addition, NZI metamaterials support nearly uniform amplitude and phase distributions, enabling simplified feeding networks and improved radiation performance. As the effective wavelength approaches infinity, phase accumulation becomes negligible, resulting in spatially uniform fields [49,51]. This is particularly advantageous for antenna arrays, as it ensures uniform excitation without complex phase or amplitude compensation, thereby reducing implementation complexity. Coherent excitation across the aperture further enhances effective aperture, gain, and radiation efficiency.

These properties, including uniform fields and geometry–frequency decoupling, naturally lead to the zeroth-order mode (ZOM) in antennas [68,69]. ZOM represents a direct manifestation of the NZI regime, featuring spatially uniform current distributions without nulls, analogous to an ideal magnetic loop. By tuning effective parameters toward near-zero values, ZOM enables resonance independent of physical size, allowing significant miniaturization while maintaining stable radiation characteristics, often with magnetic-dipole-like patterns.

3. Periodic-structure-based NZI antennas

NZI metamaterials offer powerful opportunities for electromagnetic wave engineering, but the high loss of natural plasmonic materials limits practical implementation, motivating alternative platforms. In periodic structures, the NZI condition corresponds to a near-zero propagation constant, equivalent to a zeroth-order mode. This section reviews NZI metamaterials based on periodic structures, focusing on antenna applications, as shown in Fig. 3.

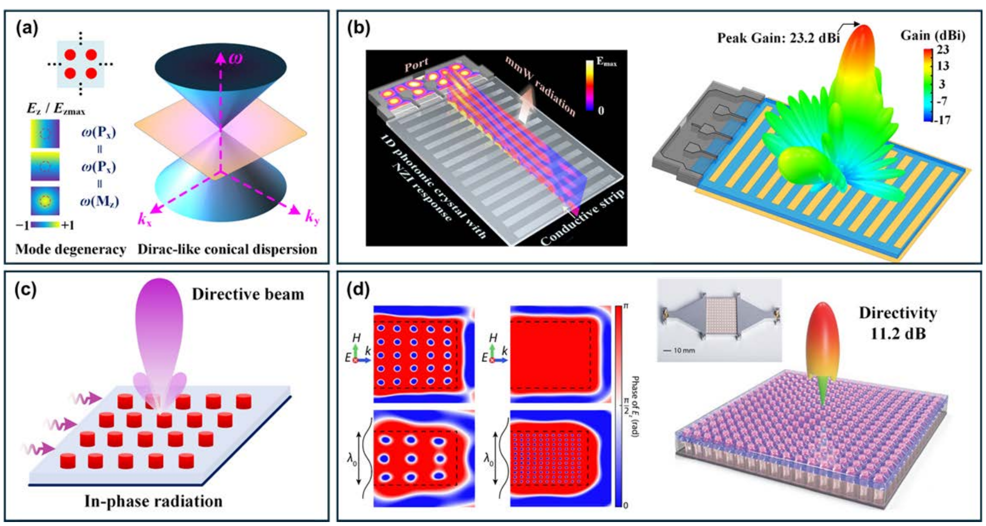

Fig. 3. Periodic-structure-based NZI antennas. (a) Illustration of the Dirac-like conical band structure of the photonic crystal at the Brillouin zone center, which exhibits an effective NZI response for directive radiation, corresponding to a near-zero propagation constant and ZOM-like behavior. (b) A high-gain NZI leaky-wave antenna constituted by planar periodic meta-gratings [77]. Reproduced with permission. Copyright 2025, IEEE. (c) In-phase radiation realized by constructing NZI photonic crystals. (d) An NZI in-phase leaky-wave antenna with a high directivity [76]. Reproduced with permission. Copyright 2024, Springer Nature.

Optical Materials EXPRESS

3.1. Periodic NZI metamaterial for leaky-wave antennas

Among artificial NZI media, periodic structures composed of meta-atoms—such as NZI photonic crystals and metamaterials [70,71] —have gained strong interest in both fundamental studies and antenna engineering. These meta-atoms can be metallic, dielectric, or hybrid, with designable lattice arrangements, enabling flexible control of effective parameters and dispersion. Through appropriate lattice engineering, the propagation constant can approach zero near specific frequencies, resulting in a stretched effective wavelength and uniform phase distribution across the structure. These unique properties provide attractive opportunities for wavefront manipulation and antenna radiation engineering. As a result, NZI responses can be realized across microwave, terahertz, and optical frequencies [15,17,20,42,43,54,70].

A key advantage of NZI photonic crystals and metamaterials in antenna engineering is the effectively stretched wavelength, which enables nearly uniform phase and amplitude excitation. As a major application, NZI-based leaky-wave antennas are first considered. Unlike phased arrays, which require individual feeds, leaky-wave antennas radiate through controlled mode leakage [72–74]. However, conventional designs suffer from an open stopband at broadside due to reflection buildup [72]. Impedance-matched NZI photonic crystals address this issue by engineering mode degeneracy to close the bandgap at the Brillouin zone center, where the propagation constant approaches zero. As shown in Fig. 3(a), a Dirac-like conical dispersion arises from the degeneracy of one monopole and two dipole modes, yielding linear dispersion, finite group velocity, and impedance matching [16]. In this regime, the near-zero propagation constant corresponds to a distributed ZOM, enabling radiation with nearly uniform phase across the structure, as illustrated in Fig. 3(c). Based on this, an 1D Dirac leaky-wave antenna using dielectric–metal hybrid cells achieves real Bloch impedance near the Γ-point, enabling continuous broadside scanning [75]. A homogeneous NZI metamaterial using high-permittivity $SrTiO_3$ further enables compact high-gain antennas approaching the directivity limit, as shown in Fig. 3(d) [76]. As shown in Fig. 3(b), an optically transparent leaky-wave antenna based on an ITO meta-grating achieves low-loss NZI propagation and over 20 dBi gain [77].

3.2. Metasurface-based NZI antennas and lenses

Besides photonic-crystal-based NZI leaky-wave antennas, metasurfaces offer an alternative platform for achieving near-zero-index responses using planar periodic structures of subwavelength resonators. Unlike bulk photonic crystals, metasurfaces realize NZI behavior by engineering surface dispersion through unit cells such as meandered lines and split-ring resonators. In the NZI regime, the effectively stretched wavelength enables phase homogenization across the aperture, transforming non-uniform excitation into a nearly uniform wavefront. This ZOM-like behavior supports metasurface-based NZI lenses for wave collimation and gain enhancement.

Tapered antennas such as Vivaldi antennas inherently support wide bandwidth and end-fire radiation. To further enhance directivity, resonant unit cells are integrated near the aperture to form NZI lenses, which can increase gain and narrow beamwidth [78–88]. For example, a meandered-line NZI lens achieved ~4 dB gain improvement at 10 GHz for a 2–14 GHz Vivaldi antenna, though enhancement at low frequencies was limited by narrow NZI bandwidth [78]. Another common approach places a metasurface-based NZI lens above broadside antennas. Unlike end-fire cases, this horizontal configuration enlarges the effective aperture, improving field collimation and directivity while maintaining high efficiency [89–96]. For example, integrating an NZI lens of ring resonators above a slot antenna yields a 7.46 dB gain improvement with 94.8% efficiency, showing minimal added loss [91]. Overall, such configurations enable efficient gain enhancement via uniform phase over an enlarged aperture.

In summary, periodic-structure-based NZI antennas achieve near-zero propagation through engineered dispersion, enabling uniform phase and amplitude distributions. Photonic-crystal implementations offer precise control of band degeneracy and impedance matching, supporting

Optical Materials EXPRESS

high-gain leaky-wave radiation while suppressing open-stopband effects. Meanwhile, metasurface-based designs extend these advantages to compact planar platforms, enabling efficient wavefront shaping and gain enhancement for both end-fire and broadside antennas.

4. Transmission-line-based NZI antennas

As another key implementation of NZI metamaterials, composite right/left-handed transmission lines (CRLH-TLs) support zeroth-order resonance through the balanced interaction of distributed inductive and capacitive loading, enabling simultaneous left- and right-handed wave propagation. At the transition frequency, the phase constant approaches zero, resulting in a nearly uniform phase distribution. Consequently, the resonance is determined primarily by the effective circuit parameters rather than the physical dimensions, relaxing the conventional relationship between frequency and size, as illustrated in Fig. 4.

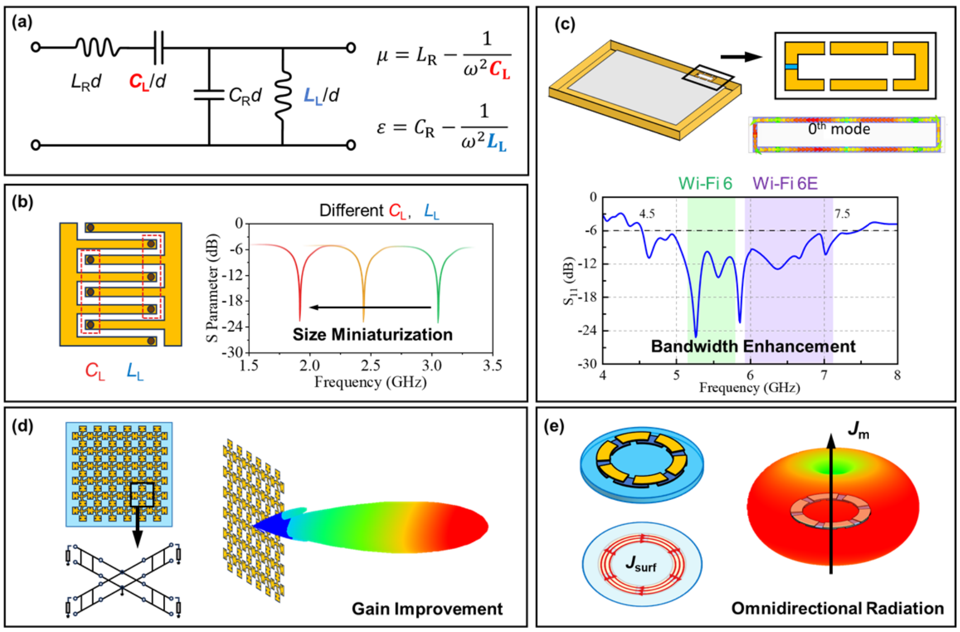

Fig. 4. Transmission-line-based NZI antennas. (a) CRLH transmission line implements NZI. (b) Compact CRLH transmission-line antenna based on a finger-connected interdigital capacitor unit cell [105]. (c) A multimode balanced NZI loop antenna integrated in a full-metal tablet housing [44]. Reproduced with permission. Copyright 2024, IEEE. (d) Pencil-beam Dirac leaky-wave antenna with NZI transmission-line grid based on CRLH-TL theory [107]. (e) Horizontally polarized omnidirectional CRLH transmission-line loop antenna array [37].

4.1. Zeroth-order modes in transmission-line structures

The concept of left-handed materials was first proposed in 1968 by Victor Veselago, who theoretically investigated media with simultaneously negative permittivity and permeability [97]. In 2003, Tatsuo Itoh and George V. Eleftheriades introduced the transmission-line approach and developed composite right/left-handed transmission line (CRLH-TL) theory [98,99]. By employing distributed circuit loading rather than resonant inclusions, CRLH-TLs enable direct dispersion engineering and support zeroth-order modes, offering reduced loss, broader bandwidth, and enhanced design flexibility. This framework has since become a foundational platform in metamaterials and antenna research [100–103].

CRLH-TLs arise from the coexistence of right- and left-handed propagation [104]. Unlike conventional right-handed media, where phase and energy flow are aligned, left-handed media exhibit antiparallel phase and group velocities. As shown in Fig. 4(a), this duality is captured by the CRLH-TL equivalent circuit, consisting of series left-handed capacitance and right-handed inductance, and shunt left-handed inductance and right-handed capacitance. The resulting dispersion relation defines right- and left-handed cutoff frequencies, as well as series and shunt resonances, with the propagation constant β transitioning from negative to positive values and crossing zero at a finite frequency, corresponding to the zeroth-order resonance. Under the balanced condition, the effective permittivity and permeability approach zero, leading to an effectively infinite wavelength and uniform phase distribution. The vanishing propagation constant reflects a balance between left- and right-handed energy storage, enabling resonance without phase accumulation and yielding field distributions independent of structural length, which provides a key advantage for electrically small antenna design.

4.2. Antenna implementations based on transmission-line NZI

Building on zeroth-order modes in transmission-line-based NZI structures, various antenna designs have exploited their dimension-independent resonance. However, this invariance mainly applies to resonant frequency, while Q factor and radiation still vary with electrical size.

As shown in Fig. 4(b), B. Zong et al. proposed a CRLH-TL-based NZI antenna using an interdigital capacitor to support ZOM, achieving over 20% size reduction [105]. Although the antennas achieve significant miniaturization, the high-Q nature limits bandwidth. To address this, coupling ZOM with conventional modes offers a route to bandwidth enhancement. References [44] and [106] demonstrated an NZI antenna for Wi-Fi 6/6E in full-metal tablet devices, as shown in Fig. 4(c). Periodically loaded structures enable ZOM at low frequencies while tuning conventional modes, achieving extended low-frequency coverage without increasing size.

Beyond bandwidth improvements, CRLH-TL-based NZI antennas enable flexible radiation control due to their uniform aperture fields, supporting directive radiation without complex feeds. High-gain designs such as Dirac leaky-wave and end-fire antennas exploit this property for coherent radiation and improved efficiency, as shown in Fig. 4(d) [107,108]. By arranging unit cells differently, diverse radiation modes can be achieved, including monopole-like and magnetic-dipole-like patterns, with stable frequency and high efficiency [36,37,109,110]. As shown in Fig. 4(e), Ref. [37] demonstrated a loop antenna operating in ZOM with nearly in-phase currents, yielding uniform loop distribution and horizontally polarized omnidirectional radiation with over 85% efficiency.

In summary, CRLH-TL theory provides a transmission-line framework for NZI antennas, enabling zeroth-order resonance with zero propagation constant at finite frequencies. This decouples resonant frequency from physical size and yields uniform field and current distributions. As a result, NZI antennas support miniaturization, bandwidth enhancement, high directivity, and radiation control, with applications in wireless communications, radar, and imaging systems.

5. Waveguide-based NZI antennas

Waveguide-based NZI antennas offer a straightforward approach to realizing near-zero-index behavior without relying on metamaterial inclusions or circuit loading. As the operating frequency approaches the waveguide cutoff, wave propagation becomes increasingly slow, leading to a vanishing propagation constant and an effective ENZ response. Under this condition, the phase remains nearly unchanged across the structure, giving rise to the excitation of the ZOM. Owing to these unique properties, waveguide-based NZI structures have been extensively employed in radiation systems and antenna feeding networks.

Optical Materials EXPRESS

The cutoff-induced ENZ response provides a new paradigm for antenna design, enabling geometry independence, frequency stability, and pattern tunability. As a representative example, Ref. [35] demonstrates a geometry-independent antenna, where the operating frequency is determined by dispersion rather than geometry, as shown in Fig. 5(a). By exploiting the effectively infinite wavelength and photonic doping for impedance matching, the antenna maintains a fixed resonant frequency under arbitrary deformations while enabling tunable far-field patterns. This behavior arises from ZOM excitation in the waveguide, characterized by uniform phase and current distribution at cutoff. This approach opens new opportunities for flexible antenna design in wireless communications and sensing applications.

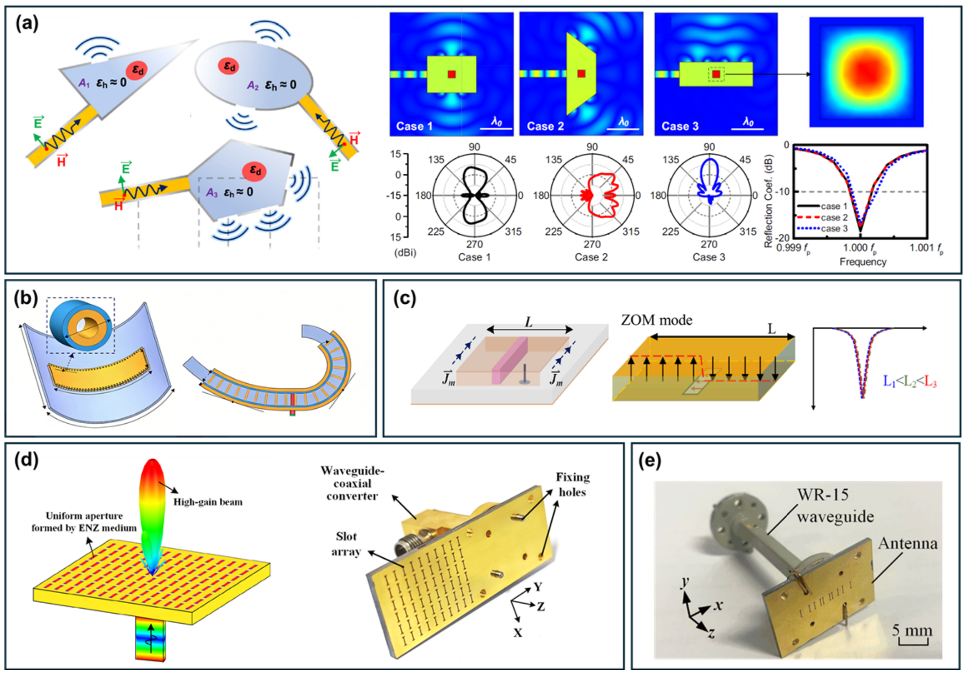

Fig. 5. Waveguide-based NZI antennas. (a) Geometry-independent ENZ antenna realized with a waveguide structure [35]. Reproduced with permission. Copyright 2022, Springer Nature. (b) Deformation-insensitive ENZ-inspired antenna employing a PDMS substrate [38]. Reproduced with permission. Copyright 2020, IEEE. (c) Photonic-doping-inspired SIW antenna with length-invariant operating frequency [113]. Reproduced with permission. Copyright 2020, IEEE. (d) Bulk-silicon MEMS-enabled planar ENZ feed network for high-gain mmWave slot arrays [51]. Copyright 2024, IEEE. (e) On-chip ENZ-assisted beam synthesis network with reduced transmission loss [49]. Reproduced with permission. Copyright 2023, Elsevier.

Waveguide-based ENZ radiation exploits dispersion near cutoff, where effective permittivity approaches zero, leading to large wavelengths and negligible phase variation. Reference [50] demonstrated an SIW-based ENZ antenna with bending-insensitive frequency and over 63% efficiency. Subsequent works extended this concept to high-gain arrays and pattern reconfiguration [46,111,112]. This approach has also been applied to flexible bioelectronic antennas, shown in Fig. 5(b) [38]. Photonic doping and anti-phase ENZ modes provide effective ways to overcome limitations of conventional ENZ waveguide antennas and enable flexible pattern control. As shown in Fig. 5(c), Ref. [113] introduces a high-permittivity dopant to create a 180° phase shift, improving directivity (~6 to ~10 dBi) and narrowing beamwidth (110° to 20%) as antenna

Optical Materials EXPRESS

length increases. Building on this, dual-polarized and compact designs have been realized using orthogonal anti-phase ENZ modes [114–116].

ENZ waveguides have been extended from radiators to low-loss, in-phase feeding and beamforming platforms, addressing feeding loss and phase errors in millimeter-wave and terahertz systems. By exploiting their quasi-static field characteristics, they provide nearly uniform amplitude and phase across multiple elements without complex feeds. This enables compact and phase-consistent designs, making them well suited for high-frequency systems.

As illustrated in Fig. 5(e), Ref. [49] employs an air-filled cutoff waveguide supporting a stair-like resonant mode for uniform-phase excitation. Subsequent works extend the feeding network to 2D arrays. Reference [117] enhances low-sidelobe designs by introducing an EMNZ medium via metallic doping of a cutoff ENZ waveguide, enabling conical amplitude tapering and uniform phase excitation without complex feeds. Reference [51] further advances 2D ENZ feeding networks using a MEMS-based architecture, as shown in Fig. 5(d), achieving 21.8 dBi gain and 92.1% aperture efficiency, highlighting strong scalability for millimeter-wave systems.

In summary, this section focuses on the advanced development of ENZ waveguide radiation and the application of ENZ waveguides as feeding networks and beam-forming platforms. These approaches highlight the potential of ENZ waveguide structures for integrated and high-performance antenna systems.

6. Conclusion and outlook

In this review, the fundamental principles and implementations of antennas based on NZI metamaterials are discussed. By exploiting the near-zero propagation constant, NZI media enable spatiotemporal decoupling, offering a unified framework to break the coupling among geometry, frequency, and radiation in conventional antennas. Within this framework, the excitation of ZOMs acts as the key mechanism, enabling geometry-independent resonance, uniform field distributions, and flexible radiation control.

Three representative platforms are reviewed: periodic-structure-based NZI metamaterials, transmission-line-based ZOM structures, and waveguide-based ENZ configurations. Despite different realizations, all rely on engineering near-zero propagation to achieve unconventional electromagnetic responses. Periodic structures enable dispersion and wavefront control, transmission-line platforms offer compact ZOM implementations, and waveguide-based approaches support low-loss, highly integrated designs for high-frequency systems. Representative NZI antennas are summarized in Table 1 and categorized by physical mechanisms. The first category involves geometry-independent resonance, enabling compact designs, bandwidth enhancement, and radiation control via zeroth-order modes. The second category is based on uniform field distribution, supporting high-gain antennas through effective aperture enhancement and improved directivity.

Nevertheless, several critical challenges remain to be addressed before NZI antennas can be widely adopted in practical systems. Inherent loss in NZI-based antennas is not solely dictated by material absorption, but is often exacerbated by strong resonant effects and high-Q operation, which enhance field confinement and increase energy dissipation, thereby limiting the overall radiation efficiency. The narrow operational bandwidth associated with strong dispersion near the NZI point poses another major obstacle for modern broadband and multi-band applications. In addition, the sensitivity of NZI responses to structural and material variations imposes stringent requirements on fabrication precision and system integration.

Looking forward, future research is expected to focus on several key directions. First, developing low-loss or active NZI platforms may help mitigate efficiency limitations and enable practical high-performance devices [48,118,119]. Second, broadband NZI responses through multi-mode coupling, dispersion engineering, or hybrid mechanisms will be essential for real-world communication systems [44,120]. Third, the integration of NZI antennas with emerging technologies such as reconfigurable systems, intelligent metasurfaces, and on-chip or

Table 1. Representative high-performance NZI-based antennas and their key characteristics

Property of NZI metamaterial	Advantages in Antenna	Reference	ZOM Method
Geometry-independent resonance behavior	Dimension miniaturization	[37]	Transmission line
		[44]	Transmission line
		[105]	Waveguide
	Radiation pattern manipulation	[50]	Waveguide
		[113]	Waveguide
Uniform field distribution	Aperture efficiency enhancement	[47]	Waveguide
		[49]	Waveguide
		[51]	Waveguide
		[77]	Periodic structure
		[107]	Transmission line

mobile platforms offers promising opportunities for multifunctional electromagnetic systems [49,121,122]. Finally, a deeper understanding of the interplay between NZI physics and antenna system-level requirements will further bridge the gap between fundamental theory and engineering applications [29,123–126].

Overall, NZI metamaterials and ZOMs provide a powerful and unifying paradigm for next-generation antenna engineering. With continued advances in materials, design methodologies, and system integration, NZI-based antennas are expected to play an increasingly important role in future wireless communication, sensing, and electromagnetic systems.

Funding. National Natural Science Foundation of China (U22B2016, 62571128, 62301162); National Key Research and Development Program of China (2021YFA0716601); Postdoctoral Fellowship Program and China Postdoctoral Science Foundation (BX20250350).

Acknowledgement. Y.L. acknowledges support from the National Natural Science Foundation of China (NSFC) Grant No. U22B2016 and National Key Research and Development Program of China Grant No. 2021YFA0716601. P. F. acknowledges support from the Postdoctoral Fellowship Program and China Postdoctoral Science Foundation Grant No. BX20250350. Z.Z. acknowledges support from Natural Science Foundation of China (NSFC) Grants No. 62571128 and No. 62301162.

Disclosures. The authors declare no conflicts of interest.

Data availability. No new data were created or analyzed in this study. Data sharing is not applicable to this article.

References

1. T. J. Cui, L. Li, S. Liu, *et al.*, "Information metamaterial systems," iScience **23**(8), 101403 (2020).
2. I. Staude and J. Schilling, "Metamaterial-inspired silicon nanophotonics," Nat. Photonics **11**(5), 274–284 (2017).
3. A. Poddubny, I. Iorsh, P. Belov, *et al.*, "Hyperbolic metamaterials," Nat. Photonics **7**(12), 948–957 (2013).
4. D. R. Smith, J. B. Pendry, and M. C. K. Wiltshire, "Metamaterials and negative refractive index," Science **305**(5685), 788–792 (2004).
5. N. Engheta, "Pursuing Near-Zero Response," Science **340**(6130), 286–287 (2013).
6. I. Liberal and N. Engheta, "Near-zero refractive index photonics," Nat. Photonics **11**(3), 149–158 (2017).
7. I. Liberal and N. Engheta, "The rise of near-zero-index technologies," Science **358**(6370), 1540–1541 (2017).
8. A. Lakhtakia, "An electromagnetic trinity from "negative permittivity" and "negative permeability"," Int. J. Infrared Millimeter Waves **23**(6), 813–818 (2002).
9. S. Enoch, G. Tayeb, P. Sabouroux, *et al.*, "A metamaterial for directive emission," Phys. Rev. Lett. **89**(21), 213902 (2002).
10. R. W. Ziolkowski, "Propagation in and scattering from a matched metamaterial having a zero index of refraction," Phys. Rev. E **70**(4), 046608 (2004).
11. Y. Li and N. Engheta, "Supercoupling of surface waves with ε-near-zero metastructures," Phys. Rev. B **90**(20), 201107 (2014).
12. M. Silveirinha and N. Engheta, "Tunneling of Electromagnetic Energy through Subwavelength Channels and Bends using ε-Near-Zero Materials," Phys. Rev. Lett. **97**(15), 157403 (2006).
13. M. G. Silveirinha and N. Engheta, "Theory of supercoupling, squeezing wave energy, and field confinement in narrow channels and tight bends using ε near-zero metamaterials," Phys. Rev. B **76**(24), 245109 (2007).

14. B. Edwards, A. Alù, M. E. Young, *et al.*, "Experimental Verification of Epsilon-Near-Zero Metamaterial Coupling and Energy Squeezing Using a Microwave Waveguide," Phys. Rev. Lett. **100**(3), 033903 (2008).
15. R. Liu, Q. Cheng, T. Hand, *et al.*, "Experimental Demonstration of Electromagnetic Tunneling Through an Epsilon-Near-Zero Metamaterial at Microwave Frequencies," Phys. Rev. Lett. **100**(2), 023903 (2008).
16. X. Huang, Y. Lai, Z. H. Hang, *et al.*, "Dirac cones induced by accidental degeneracy in photonic crystals and zero-refractive-index materials," Nat. Mater. **10**(8), 582–586 (2011).
17. Y. Li, S. Kita, P. Muñoz, *et al.*, "On-chip zero-index metamaterials," Nat. Photonics **9**(11), 738–742 (2015).
18. D. I. Vulis, Y. Li, O. Reshef, *et al.*, "Monolithic CMOS-compatible zero-index metamaterials," Opt. Express **25**(11), 12381–12399 (2017).
19. I. Liberal and N. Engheta, "Nonradiating and radiating modes excited by quantum emitters in open epsilon-near-zero cavities," Sci. Adv. **2**(10), e1600987 (2016).
20. R. Maas, J. Parsons, N. Engheta, *et al.*, "Experimental realization of an epsilon-near-zero metamaterial at visible wavelengths," Nat. Photonics **7**(11), 907–912 (2013).
21. O. Reshef, P. Camayd-Muñoz, D. I. Vulis, *et al.*, "Integrated Zero-Index Metamaterials and Waveguides," in *Integrated Photonics Research, Silicon and Nanophotonics*, (Optica Publishing Group, 2018), ITh3J.3.
22. M. Silveirinha and N. Engheta, "Design of matched zero-index metamaterials using nonmagnetic inclusions in epsilon-near-zero media," Phys. Rev. B **75**(7), 075119 (2007).
23. I. Liberal, A. M. Mahmoud, Y. Li, *et al.*, "Photonic doping of epsilon-near-zero media," Science **355**(6329), 1058–1062 (2017).
24. M. Coppolaro, M. Moccia, G. Castaldi, *et al.*, "Non-Hermitian doping of epsilon-near-zero media," Proc. Natl. Acad. Sci. **117**(25), 13921–13928 (2020).
25. I. Liberal, Y. Li, and N. Engheta, "Reconfigurable epsilon-near-zero metasurfaces via photonic doping," Nanophotonics **7**(6), 1117–1127 (2018).
26. Z. Zhou, Y. Li, H. Li, *et al.*, "Substrate-integrated photonic doping for near-zero-index devices," Nat. Commun. **10**(1), 4132 (2019).
27. I. Liberal, M. Lobet, Y. Li, *et al.*, "Near-zero-index media as electromagnetic ideal fluids," Proc. Natl. Acad. Sci. **117**(39), 24050–24054 (2020).
28. H. Li, Z. Zhou, W. Sun, *et al.*, "Direct observation of ideal electromagnetic fluids," Nat. Commun. **13**(1), 4747 (2022).
29. W. Yan, H. Li, X. Qin, *et al.*, "Fano resonance in epsilon-near-zero media," Phys. Rev. Lett. **133**(25), 256402 (2024).
30. A. M. Mahmoud and N. Engheta, "Wave–matter interactions in epsilon-and-mu-near-zero structures," Nat. Commun. **5**(1), 5638 (2014).
31. A. Alù and N. Engheta, "Light squeezing through arbitrarily shaped plasmonic channels and sharp bends," Phys. Rev. B **78**(3), 035440 (2008).
32. A. Alù, M. G. Silveirinha, N. Engheta, *et al.*, "Transmission-line analysis of ε-near-zero–filled narrow channels," Phys. Rev. E **78**(1), 016604 (2008).
33. Y. Li, I. Liberal, C. Della Giovampaola, *et al.*, "Waveguide metatronics: Lumped circuitry based on structural dispersion," Sci. Adv. **2**(6), e1501790 (2016).
34. I. Liberal, A. M. Mahmoud, N. Engheta, *et al.*, "Geometry-invariant resonant cavities," Nat. Commun. **7**(1), 10989 (2016).
35. H. Li, Z. Zhou, Y. He, *et al.*, "Geometry-independent antenna based on Epsilon-near-zero medium," Nat. Commun. **13**(1), 3568 (2022).
36. K. Wei, Z. Zhang, Z. Feng, *et al.*, "A Wideband MNG-TL Dipole Antenna With Stable Radiation Patterns," IEEE Trans. Antennas Propag. **61**(5), 2418–2424 (2013).
37. K. Wei, Z. Zhang, Z. Feng, *et al.*, "A MNG-TL Loop Antenna Array With Horizontally Polarized Omnidirectional Patterns," IEEE Trans. Antennas Propag. **60**(6), 2702–2710 (2012).
38. Z. Hu, C. Chen, Z. Zhou, *et al.*, "An epsilon-near-zero-inspired PDMS substrate antenna with deformation-insensitive operating frequency," Antennas Wirel. Propag. Lett. **19**(9), 1591–1595 (2020).
39. J. A. Stratton and L. Chu, "Diffraction theory of electromagnetic waves," Phys. Rev. **56**(1), 99–107 (1939).
40. P. M. T. Ikonen, K. N. Rozanov, A. V. Osipov, *et al.*, "Magnetodielectric substrates in antenna miniaturization: Potential and limitations," IEEE Trans. Antennas Propag. **54**(11), 3391–3399 (2006).
41. T. A. Milligan, *Modern Antenna Design* (John Wiley & Sons, 2005).
42. E. Forati, G. W. Hanson, D. F. Sievenpiper, *et al.*, "An epsilon-near-zero total-internal-reflection metamaterial antenna," IEEE Trans. Antennas Propag. **63**(5), 1909–1916 (2015).
43. C. Xu, J. Shi, X. Liu, *et al.*, "Deterministic Double-Zero Media and Robust Wave Manipulation Using a Phononic Weyl Semimetal," Phys. Rev. Lett. **135**(4), 046902 (2025).
44. W. Yan, Y. Zhang, K. Li, *et al.*, "Multimode balanced mu-near-zero loop antenna for Wi-Fi 6/6E applications in full metal housing tablet computers," IEEE Trans. Antennas Propag. **72**(7), 5469–5478 (2024).
45. J. Kim, G. Kim, W. Seong, *et al.*, "A tunable internal antenna with an epsilon negative zeroth order resonator for DVB-H service," IEEE Trans. Antennas Propag. **57**(12), 4014–4017 (2009).
46. Z. Liu, Z. Zhou, Y. Li, *et al.*, "Integrated epsilon-near-zero antenna for omnidirectional radiation," Appl. Phys. Lett. **119**(15), 151904 (2021).

Optical Materials EXPRESS

47. H. Li and Y. Li, "Low-sidelobe antenna array based on evanescent mode of cutoff waveguide," IEEE Trans. Antennas Propag. **70**(12), 11608–11616 (2022).
48. W. Yan, Z. Zhou, H. Li, *et al.*, "Low-Loss Epsilon-Near-Zero Metamaterials," Laser Photonics Rev. **17**(8), 2201000 (2023).
49. H. Li, Z. Zhou, Y. Zhao, *et al.*, "Low-loss beam synthesizing network based on Epsilon-near-zero (ENZ) medium for on-chip antenna array," Chip **2**(2), 100049 (2023).
50. Z. Zhou and Y. Li, "Effective epsilon-near-zero (ENZ) antenna based on transverse cutoff mode," IEEE Trans. Antennas Propag. **67**(4), 2289–2297 (2019).
51. Y. Zhang, H. Li, Y. Zhao, *et al.*, "2-D epsilon-near-zero (ENZ) feeding network for high-gain millimeter-wave slot antenna array using bulk silicon MEMS technology," IEEE Trans. Antennas Propag. **72**(4), 3055–3063 (2024).
52. J. D. Jackson, *Classical Electrodynamics* (John Wiley & Sons, 2012).
53. A. Ciattoni, A. Marini, C. Rizza, *et al.*, "Polariton excitation in epsilon-near-zero slabs: Transient trapping of slow light," Phys. Rev. A **87**(5), 053853 (2013).
54. R.-Y. Zhang, X. Cui, Y.-S. Zeng, *et al.*, "Bulk–spatiotemporal vortex correspondence in gyromagnetic zero-index media," Nature **641**(8065), 1142–1148 (2025).
55. A. Alu and N. Engheta, "Coaxial-to-Waveguide Matching With ε-Near-Zero Ultranarrow Channels and Bends," IEEE Trans. Antennas Propag. **58**(2), 328–339 (2010).
56. E. J. R. Vesseur, T. Coenen, H. Caglayan, *et al.*, "Experimental verification of n= 0 structures for visible light," Phys. Rev. Lett. **110**(1), 013902 (2013).
57. Z. Zhou and Y. Li, "N-port equal/unequal-split power dividers using epsilon-near-zero metamaterials," IEEE Trans. Microwave Theory Tech. **69**(3), 1529–1537 (2021).
58. Z. Zhou, Y. Li, E. Nahvi, *et al.*, "General impedance matching via doped epsilon-near-zero media," Phys. Rev. Appl. **13**(3), 034005 (2020).
59. Z. Zhou, H. Li, W. Sun, *et al.*, "Dispersion coding of ENZ media via multiple photonic dopants," Light: Sci. Appl. **11**(1), 207 (2022).
60. I. Liberal and N. Engheta, "Manipulating thermal emission with spatially static fluctuating fields in arbitrarily shaped epsilon-near-zero bodies," Proc. Natl. Acad. Sci. **115**(12), 2878–2883 (2018).
61. I. Liberal, Y. Li, and N. Engheta, "Magnetic field concentration assisted by epsilon-near-zero media," Phil. Trans. R. Soc. A. **375**(2090), 20160059 (2017).
62. P. Moitra, Y. Yang, Z. Anderson, *et al.*, "Realization of an all-dielectric zero-index optical metamaterial," Nat. Photonics **7**(10), 791–795 (2013).
63. I. Liberal and N. Engheta, "Zero-index structures as an alternative platform for quantum optics," Proc. Natl. Acad. Sci. **114**(5), 822–827 (2017).
64. M. Lobet, I. Liberal, E. N. Knall, *et al.*, "Fundamental radiative processes in near-zero-index media of various dimensionalities," ACS Photonics **7**(8), 1965–1970 (2020).
65. N. Engheta, "150 years of Maxwell's equations," Science **349**(6244), 136–137 (2015).
66. A. Alù, M. G. Silveirinha, A. Salandrino, *et al.*, "Epsilon-near-zero metamaterials and electromagnetic sources: Tailoring the radiation phase pattern," Phys. Rev. B **75**(15), 155410 (2007).
67. W. Yan, Y. Zhang, H. Li, *et al.*, "Two-dimensional Low-Sidelobe Millimeter-wave On-chip Antenna Array Based on ENZ-Evanescent Hybrid Modes," in *2024 International Conference on Microwave and Millimeter Wave Technology (ICMMT)*, (2024), 1–3.
68. C. A. Balanis, *Antenna Theory: Analysis and Design* (John Wiley & Sons, 2016).
69. J.-H. Park, Y.-H. Ryu, J.-H. Lee, *et al.*, "Mu-Zero Resonance Antenna," IEEE Trans. Antennas Propag. **58**(6), 1865–1875 (2010).
70. Y. Li, C. T. Chan, E. Mazur, *et al.*, "Dirac-like cone-based electromagnetic zero-index metamaterials," Light: Sci. Appl. **10**(1), 203 (2021).
71. J. Luo and Y. Lai, "Hermitian and non-Hermitian Dirac-like cones in photonic and phononic structures," Front. Phys. **10**, 845624 (2022).
72. W. Zhou, J. Liu, Y. Long, *et al.*, "Investigation of shorting vias for suppressing the open stopband in an SIW periodic leaky-wave structure," IEEE Trans. Microwave Theory Tech. **66**(6), 2936–2945 (2018).
73. Z. Zhou, Y. Zhang, Y. Zheng, *et al.*, "The low-attenuation endfire leaky-wave state on an optically transparent lossy film," Engineering **43**, 72–80 (2024).
74. X. Zheng, Y. Ge, G. Li, *et al.*, "Efficient Analytical Design Strategy for High-Gain Nonresonant Partially-Reflective-Surface Antennas," Antennas Wirel. Propag. Lett. **24**(4), 898–902 (2025).
75. M. Memarian and G. V. Eleftheriades, "Dirac leaky-wave antennas for continuous beam scanning from photonic crystals," Nat. Commun. **6**(1), 5855 (2015).
76. Y. Liu, T. Dong, X. Qin, *et al.*, "High-permittivity ceramics enabled highly homogeneous zero-index metamaterials for high-directivity antennas and beyond," eLight **4**(1), 4 (2024).
77. Z. Zhou, Y. Zhang, Z. Kuang, *et al.*, "An Optically Transparent Near-Zero-Index Grating Metamaterial for Enhanced On-Glass Millimeter-Wave Radiation," IEEE Trans. Antennas Propag. **73**(6), 4092–4097 (2025).
78. B. Zhou and T. J. Cui, "Directivity enhancement to Vivaldi antennas using compactly anisotropic zero-index metamaterials," Antennas Wirel. Propag. Lett. **10**, 326–329 (2011).

79. M. Bhaskar, E. Johari, Z. Akhter, *et al.*, "Gain enhancement of the Vivaldi antenna with band notch characteristics using zero-index metamaterial," Microw. Opt. Technol. Lett. **58**(1), 233–238 (2016).
80. M. T. Islam, M. Samsuzzaman, S. Kibria, *et al.*, "Metasurface loaded high gain antenna based microwave imaging using iteratively corrected delay multiply and sum algorithm," Sci. Rep. **9**(1), 17317 (2019).
81. M. Sun, Z. N. Chen, and X. Qing, "Gain enhancement of 60-GHz antipodal tapered slot antenna using zero-index metamaterial," IEEE Trans. Antennas Propag. **61**(4), 1741–1746 (2013).
82. L. Guo, H. Yang, Q. Zhang, *et al.*, "A compact antipodal tapered slot antenna with artificial material lens and reflector for GPR applications," IEEE Access **6**, 44244–44251 (2018).
83. R.-C. Deng, X.-m. Yang, B. Ma, *et al.*, "Performance enhancement of novel antipodal Vivaldi antenna with irregular spacing distance slots and modified-w-shaped metamaterial loading," Appl. Phys. A **125**(1), 5 (2019).
84. M.-A. Boujemaa, R. Herzi, F. Choubani, *et al.*, "UWB Antipodal Vivaldi antenna with higher radiation performances using metamaterials," Appl. Phys. A **124**(10), 714 (2018).
85. S. El-Nady, H. M. Zamel, M. Hendy, *et al.*, "Gain enhancement of a millimeter wave antipodal vivaldi antenna by epsilon-near-zero metamaterial," Progress In Electromagnetics Research C **85**, 105–116 (2018).
86. D. Ramaccia, F. Scattone, F. Bilotti, *et al.*, "Broadband compact horn antennas by using EPS-ENZ metamaterial lens," IEEE Trans. Antennas Propag. **61**(6), 2929–2937 (2013).
87. W. Cao, B. Zhang, A. Liu, *et al.*, "Gain enhancement for broadband periodic endfire antenna by using split-ring resonator structures," IEEE Trans. Antennas Propag. **60**(7), 3513–3516 (2012).
88. R. E. A. Shehata, A. Elboushi, M. Hindy, *et al.*, "Metamaterial inspired LPDA MIMO array for upper band 5G applications," Int. J. RF Mic. Comp-Aid. Eng. **32**(8), e23212 (2022).
89. S. V. Nandigama, B. Kunooru, D. Ramakrishna, *et al.*, "Pattern Similarity and Gain Enhancement of Dual-Band Antenna Using an ENZ Metamaterial," J. Electromagn. Eng. Sci. **23**(6), 461–469 (2023).
90. J. Ju, D. Kim, W. J. Lee, *et al.*, "Wideband high-gain antenna using metamaterial superstrate with the zero refractive index," Microw. Opt. Technol. Lett. **51**(8), 1973–1976 (2009).
91. T. Shaw, D. Bhattacharjee, D. Mitra, *et al.*, "Gain enhancement of slot antenna using zero-index metamaterial superstrate," Int. J. RF Mic. Comp-Aid. Eng. **27**(4), e21078 (2017).
92. A. H. Abdelgwad and T. M. Said, "High performance microstrip monopole antenna with loaded metamaterial wire medium superstrate," Int. J. RF Mic. Comp-Aid. Eng. **29**(5), e21557 (2019).
93. R. Mark, H. V. Singh, K. Mandal, *et al.*, "Mutual coupling reduction using near-zero ε and μ metamaterial-based superstrate for an MIMO application," IET Microwaves, Antennas & Prop. **14**(6), 479–484 (2020).
94. P. Usha and C. Krishnan, "Epsilon near zero metasurface for ultrawideband antenna gain enhancement and radar cross section reduction," AEU-International Journal of Electronics and Communications **119**, 153167 (2020).
95. C. Cheng, Y. Lu, D. Zhang, *et al.*, "Gain enhancement of terahertz patch antennas by coating epsilon-near-zero metamaterials," Superlattices Microstruct. **139**, 106390 (2020).
96. A. Bakhtiari, "Investigation of enhanced gain miniaturized patch antenna using near zero index metamaterial structure characteristics," IETE Journal of research **68**(2), 1312–1319 (2022).
97. V. Veselago, "The electrodynamics of substances with simultaneously negative values of and," Usp. fiz. nauk **92**(7), 517–526 (1967).
98. C. Caloz and T. Itoh, "Application of the transmission line theory of left-handed (LH) materials to the realization of a microstrip" LH line"," in *IEEE Antennas and Propagation Society International Symposium (IEEE Cat. No. 02CH37313)*, (IEEE, 2002), 412–415.
99. G. V. Eleftheriades, A. K. Iyer, and P. C. Kremer, "Planar negative refractive index media using periodically LC loaded transmission lines," IEEE Trans. Microwave Theory Tech. **50**(12), 2702–2712 (2002).
100. C. Wang, B.-J. Hu, and X.-Y. Zhang, "Compact triband patch antenna with large scale of frequency ratio using CRLH-TL structures," Antennas Wirel. Propag. Lett. **9**, 744–747 (2010).
101. H. Lee, D.-J. Woo, and S. Nam, "Compact and bandwidth-enhanced asymmetric coplanar waveguide (ACPW) antenna using CRLH-TL and modified ground plane," Antennas Wirel. Propag. Lett. **15**, 810–813 (2016).
102. J. Zhang, S. Yan, and G. A. E. Vandenbosch, "Radial CRLH-TL-based dual-band antenna with frequency agility," IEEE Trans. Antennas Propag. **68**(7), 5664–5669 (2020).
103. J. Zhang, S. Yan, and G. A. E. Vandenbosch, "Realization of dual-band pattern diversity with a CRLH-TL-inspired reconfigurable metamaterial," IEEE Trans. Antennas Propag. **66**(10), 5130–5138 (2018).
104. A. Sanada, C. Caloz, and T. Itoh, "Characteristics of the composite right/left-handed transmission lines," IEEE Microw. Wireless Compon. Lett. **14**(2), 68–70 (2004).
105. B.-F. Zong, G.-M. Wang, Y.-W. Wang, *et al.*, "Compact antenna using finger-connected interdigital capacitor-based composite right/left-handed transmission-line unit cell," IEEE Trans. Antennas Propag. **64**(5), 1994–1999 (2016).
106. K. Li, W. Yan, Y. Zhang, *et al.*, "Metal Shell Effect on Multi-Mode Antennas for Wideband Mobile Applications," IEEE Trans. Antennas Propag. **73**(11), 8621–8630 (2025).
107. A. H. Dorrah and G. V. Eleftheriades, "Pencil-beam single-point-fed Dirac leaky-wave antenna on a transmission-line grid," Antennas Wirel. Propag. Lett. **16**, 545–548 (2017).
108. H. Li, Y. Li, L. Chang, *et al.*, "A wideband dual-polarized endfire antenna array with overlapped apertures and small clearance for 5G millimeter-wave applications," IEEE Trans. Antennas Propag. **69**(2), 815–824 (2021).
109. J.-H. Park, Y.-H. Ryu, J.-G. Lee, *et al.*, "Epsilon negative zeroth-order resonator antenna," IEEE Trans. Antennas Propag. **55**(12), 3710–3712 (2007).

Optical Materials EXPRESS

110. J.-Q. Huang and Q.-X. Chu, "Small ZOR antenna with high efficiency based on epsilon negative transmission line," in *2010 International Conference on Microwave and Millimeter Wave Technology*, (IEEE, 2010), 1905–1907.
111. D. M. George, A. Chandroth, C. C. H. Ng, *et al.*, "High-gain narrow-band slotted antenna based on ENZ SIW structure," J. Phys. D: Appl. Phys. **51**(13), 135102 (2018).
112. D. M. George and A. Chandroth, "5GHz high gain slotted SIW epsilon near zero antenna array for wireless communications," Eng. Res. Express **2**(4), 045014 (2020).
113. Z. Zhou and Y. Li, "A photonic-doping-inspired SIW antenna with length-invariant operating frequency," IEEE Trans. Antennas Propag. **68**(7), 5151–5158 (2020).
114. H. Li, Z. Zhou, and Y. Li, "Length-irrelevant dual-polarized antenna based on antiphase epsilon-near-zero mode," IEEE Trans. Antennas Propag. **70**(1), 720–725 (2022).
115. Y. Zhang, P. Li, X. Qin, *et al.*, "Dual-polarized microstrip antenna with single-dimension-constraint resonant frequency," IEEE Trans. Antennas Propag. **72**(11), 8365–8374 (2024).
116. Z. Liu, Y. Zhang, W. Sun, *et al.*, "Low-profile epsilon-near-zero (ENZ) cavity antenna array for wide-angle beam scanning," Antennas Wirel. Propag. Lett. **23**(7), 2115–2119 (2024).
117. J. Li, L. Zhao, and H. Wu, "A novel highly directional antenna array based on epsilon-mu-near-zero (EMNZ) with air-gap structure," IEEE Trans. Antennas Propag. **73**(4), 2357–2368 (2025).
118. E. Ozturk, H. Asif, M. Gunay, *et al.*, "Active tuning of ENZ resonances in a meta-antenna through phase modulation of an optical pulse," J. Opt. Soc. Am. B **43**(3), 375–379 (2026).
119. S. Hraba, I. Krois, I. Bonic, *et al.*, "Broadband epsilon-near-zero (ENZ) and mu-near-zero (MNZ) active metamaterial," (2011).
120. P. Fu, P. Li, and Y. Li, "Bandwidth Enhancement of Epsilon-Near-Zero Supercoupling with Inverse-Designed Metamaterials," Laser Photonics Rev. **19**(9), 2402014 (2025).
121. W. Jia, G. Saerens, Ü.-L. Talts, *et al.*, "Polarization-entangled Bell state generation from an epsilon-near-zero metasurface," Sci. Adv. **11**(8), eads3576 (2025).
122. W. Jia, C. Gao, Y. Zhao, *et al.*, "Intracavity spatiotemporal metasurfaces," Adv. Photonics **5**(02), 026002 (2023).
123. W. Yan, P. Li, K. Li, *et al.*, "Extreme electromagnetic absorption in epsilon-near-zero media," Phys. Rev. B **113**(3), 035104 (2026).
124. L. Ruks and J. Ruostekoski, "Emergence of an Epsilon-Near-Zero Medium from Microscopic Atomic Principles," Phys. Rev. Lett. **135**(23), 233603 (2025).
125. Y. Zhou, Y. Wang, S. Qiu, *et al.*, "Microscopic response mechanism of epsilon-negative and epsilon-near-zero metacomposites," Research **8**, 0556 (2025).
126. Y. Kiasat, M. G. Donato, M. Hinczewski, *et al.*, "Epsilon-near-zero (ENZ)-based optomechanics," Commun. Phys. **6**(1), 69 (2023).